X-621-68-160
PREPRINT

NASA TM X-63224

THE UPPER ATMOSPHERE AS A MULTIPLE REFRACTIVE MEDIUM FOR NEUTRAL AIR MOTIONS

H. VOLLAND

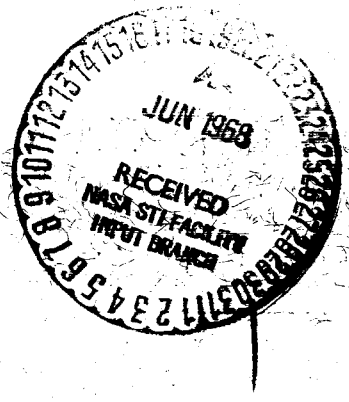

MAY 1968

GSFC — GODDARD SPACE FLIGHT CENTER —

GREENBELT, MARYLAND

X-621-68-160

THE UPPER ATMOSPHERE AS A MULTIPLE REFRACTIVE MEDIUM FOR NEUTRAL AIR MOTIONS

H. Volland*

May 1968

GODDARD SPACE FLIGHT CENTER
Greenbelt, Maryland

*On leave from the Astronomical Institutes of the University of Bonn, Germany, as a National Academy of Sciences–National Research Council Associate with the National Aeronautics and Space Administration.

THE UPPER ATMOSPHERE AS A MULTIPLE REFRACTIVE MEDIUM FOR NEUTRAL AIR MOTIONS

H. Volland

ABSTRACT

Under the influence of gravity and heat conduction four plane characteristic waves obliquely incident on a horizontally stratified atmosphere can propagate, two of them upward and the two other downward. The two pairs of characteristic waves are the well known acoustic-gravity waves and the heat conduction waves. Molecular viscosity generates two further pairs of characteristic waves, the ordinary and the extraordinary viscosity waves. Ion drag and Coriolis force make the atmosphere anisotropic with respect to the characteristic waves. Their propagation characteristics for east to west and north to south propagation differ from each other.

Some analytical solutions of the eigenvalues of these eight characteristic waves are given in this paper. Numerical calculations of the eigenvalues depending on the parameters of the thermosphere, on frequency, azimuth and on angle of incidence are presented and discussed in some detail.

CONTENTS

THE UPPER ATMOSPHERE AS A MULTIPLE REFRACTIVE MEDIUM FOR NEUTRAL AIR MOTIONS

I. INTRODUCTION

Since the work of Harris and Priester (1962) and of Hines (1960) it is well established that neutral air waves propagate within the thermosphere driven either by the solar EUV heat input within the thermosphere or originating in the lower atmosphere and propagating upward into the thermosphere. The paper of Harris and Priester stressed the importance of heat conductivity for the propagation characteristics of the diurnal waves. This is due to the fact that the ratio

$$\kappa / \overline{\rho}$$

(κ = coefficient of heat conductivity; $\overline{\rho}$ = mean density) is increasing with height because κ depends only on temperature while $\overline{\rho}$ decreases exponentially with altitude. The change in the propagation behavior of gravity waves due to heat conduction and viscosity has been shown by Pitteway and Hines (1963). They calculated the eigenvalues of plane harmonic gravity waves and discussed the energy dissipation of these waves due to heat conduction and viscosity. Midgley and Liemohn (1966) made a full wave calculation of neutral atmospheric waves below 160 km altitude taking into account heat conduction and viscosity. They used a numerical technique to suppress the evanescent heat conduction waves and viscosity waves and calculated reflection coefficients of the lower atmosphere with respect to gravity waves.

More recent observations of traveling ionospheric disturbances (TID) made by Thome (1964) and Georges (1967) and observations of wave like structure in the thermospheric neutral density by Newton et al. (1968) show that gravity waves can reach altitudes as high as 500 km. At these heights however heat conduction waves and viscosity waves are no longer evanescent waves compared with gravity waves and may play a more or less important role.

In order to deal with either the ray treatment or the full wave treatment of atmospheric waves one has to know the eigenvalues of the different wave modes. In this paper analytical and numerical calculations of the dispersion equation valid at thermospheric heights will be presented. For convenience we restrict ourselves to the simplest type of waves, namely plane harmonic nonducted

neutral atmospheric waves propagating obliquely through a horizontally stratified quiet atmosphere under the influence of heat conduction, viscosity, ion drag and Coriolis force. Under those conditions four pairs of characteristic waves exist:

a. Acoustic-gravity waves

b. Heat conduction waves

c. Ordinary viscosity waves

d. Extraordinary viscosity waves.

Characteristic waves are only well defined within a homogeneous medium. The atmosphere however behaves like an inhomogeneous medium with respect to neutral air waves because the eigenvalues of the characteristic waves are functions of

$$\frac{\kappa}{\bar{p}} \text{ and } \frac{\eta}{\bar{p}} \tag{1}$$

κ = coefficient of heat conductivity

η = coefficient of viscosity

$\bar{p}$ = mean pressure

This leads to the construction of a model atmosphere consisting of a number of homogeneous slabs of constant temperature and constant parameters $\kappa/\bar{p}$ and $\eta/\bar{p}$. In each of these slabs the eight characteristic waves propagate uncoupled from each other. Coupling then occurs only at the boundary between adjacent slabs with different parameters.

In this paper we shall solve the eigenvalue equation of the characteristic waves analytically and numerically within one homogeneous slab. We shall discuss the behavior of the eigenvalues of the different wave modes as functions of angle of incidence, frequency and thermospheric parameters. The validity of such model atmosphere in full wave and ray treatments has been demonstrated in an additional paper (Volland, 1968).

II. THE BASIC EQUATIONS

We start from the equations of conservation of mass, momentum and energy and the ideal gas equation of the neutral gas which are

$$\frac{\partial \rho}{\partial t} + \operatorname{div}(\rho \vec{v}) = 0$$

$$\rho \frac{d\vec{v}}{dt} + \operatorname{div} \sigma + \nu \rho (\vec{v} - \vec{v}_i) - 2\vec{\Omega} \times \vec{v} \rho + \operatorname{grad} p - \rho \vec{g} = 0 \tag{2}$$

$$c_v \rho \frac{dT}{dt} + p \operatorname{div} \vec{v} + \beta - \operatorname{div}(\kappa \operatorname{grad} T) + \nu \rho \vec{v} \cdot (\vec{v} - \vec{v}_i) = 0$$

$$p - \mu \rho T = 0.$$

ρ density; $\vec{v} = (u, v, w)$ velocity

p pressure; T temperature

ν collision frequency between ions and one molecule

σ viscous stress tensor

$$\sigma_{ik} = -\eta \left\{ \frac{\partial v_i}{\partial x_k} + \frac{\partial v_k}{\partial x_i} - \frac{2}{3} \delta_{ik} \operatorname{div} \vec{v} \right\} \text{ element of } \sigma$$

η coefficient of molecular viscosity

$\vec{\Omega}$ earth's rotational vector

$\vec{g}$ gravitational acceleration force

c_v specific heat at constant volume

$$\vec{v}_i = \frac{(\vec{v} \cdot \vec{B}_0)\, \vec{B}_0}{B_0^2}$$

ion velocity parallel to the geomagnetic field $\vec{B}_0$

$$\beta = \sum_i \sum_k \sigma_{ik} \frac{\partial v_i}{\partial x_k}$$

viscosity heating

κ coefficient of heat conductivity

$\mu = \tilde{R}/M$

$\tilde{R}$ gas constant

M molecular weight

For solving the system of Equations (2) a consequent perturbation method is applied assuming that the time independent mean values like density $\bar{\rho}$, pressure $\bar{p}$ and temperature $\bar{T}$ are already known and that the mean velocity of the air $\bar{v}$ is zero. The perturbation is considered to be a plane harmonic nonducted wave of angular frequency ω and of wave number k obliquely incident on a horizontally stratified plane atmosphere in which all parameters depend only on the vertical component z. Then all variables are functions of the coordinates x, y, z, and time t according to

$$f(z)\, e^{j\omega t - jk \sin\theta (x \cos\Lambda + y \sin\Lambda)}. \tag{3}$$

θ is the angle of incidence and Λ is the azimuth of the plane of incidence of the wave with respect to geographic south. We assume that no internal energy source exists.

The vertical component of energy transported by the different wave modes is continuous at any internal boundary. This implies the equivalence to Snell's law:

$$\begin{aligned} k \sin\theta &= \text{const.} \\ \Lambda &= \text{const.} \end{aligned} \tag{4}$$

We normalize wavenumber k by an arbitrary constant wavenumber

$$k_0 = \frac{\omega}{C_0} \tag{5}$$

where

$$C_0 = \sqrt{\gamma \mu T_0} \tag{6}$$

is the acoustic phase velocity at an arbitrary height z_0. Since we exclude ducted wave modes, our model atmosphere is extended infinitely in vertical direction. Thus the normalized horizontal wavenumbers

$$\frac{k_x}{k_0} = S_0 \cos \Lambda_0$$

$$\frac{k_y}{k_0} = S_0 \sin \Lambda_0$$

can have all possible real values and remain constant throughout the whole atmosphere.

For convenience we rotate the coordinate system in such a manner that the new x-axis points in the Λ_0 direction. Then the horizontal components of the velocity with respect to the new coordinate system are

$$\begin{aligned} \tilde{u} &= u \cos \Lambda_0 + v \sin \Lambda_0 \\ \tilde{v} &= -u \sin \Lambda_0 + v \cos \Lambda_0 \end{aligned} \tag{7}$$

The values $\Delta\tilde{u}$, $\Delta\tilde{v}$, Δw, Δp, $\Delta\rho$ and ΔT are the deviations from the mean values and are considered to be small compared with C_0, $\bar{p}(z)$, $\bar{\rho}(z)$ and $\bar{T}(z)$ of the quiet atmosphere. Thus all products of these small values can be neglected. We normalize these variables according to

$$e_1 = \frac{\Delta w}{C_0};\ e_3 = \frac{\Delta T}{\bar{T}};\ e_5 = \frac{\Delta \tilde{u}}{C_0};\ e_7 = \frac{\Delta \tilde{v}}{C_0}$$

$$e_2 = \frac{\Delta p}{\bar{p}};\ e_4 = \frac{\kappa \Delta T'}{C_0 \bar{p}};\ e_6 = \frac{\Delta \tilde{u}'}{\omega};\ e_8 = \frac{\Delta \tilde{v}'}{\omega} \tag{8}$$

The derivative with respect to z has been replaced by a prime ($\partial/\partial z = '$).

Introducing the expressions of Equation (8) into the system of Equations (2) and considering the time and spatial dependence of Equation (3) the variables $\Delta w''$ and $\Delta \rho$ can be eliminated which leads to a system of first order differential equations which in concise matrix form is

$$\mathbf{e}' - jk_0 \mathbf{K}\mathbf{e} = \mathbf{0}, \tag{9}$$

where

$$\mathbf{e}(z) = \begin{pmatrix} e_1 \\ \cdot \\ \cdot \\ \cdot \\ e_8 \end{pmatrix}$$

is the column matrix containing the 8 independent variables defined in Equation (8). The coefficient matrix

$$\mathbf{K} = \begin{pmatrix} \mathbf{K}_1 & \mathbf{K}_2 \\ \mathbf{K}_3 & \mathbf{K}_4 \end{pmatrix} \tag{10}$$

has the submatrices

$$K_1 = \begin{pmatrix} -2jA_1 & -1 & 1 & 0 \\ -\gamma(1-\delta D)d_1 & 2j(A_1-A_2)\delta & -2j(A-A_2\delta) & -\frac{2jG\delta}{d_2} \\ 0 & 0 & 2j(A_1-A) & -\frac{2jG}{d_2} \\ -2jd_2\left(A_1-\frac{A}{\gamma}\right) & -1 & d_2\left(1-\frac{jS_0^2}{2G}\right) & -2jA \end{pmatrix}$$

$$K_2 = \begin{pmatrix} S_0 & 0 & 0 & 0 \\ -\delta\left(2A_1S_0j - 3A_2S_0j + \frac{3}{4}RB_1d_1\right) & -\frac{3S_0\delta j}{4} & -\frac{3R\delta B_4 d_1}{4} & 0 \\ 0 & 0 & 0 & 0 \\ 0 & 0 & 0 & 0 \end{pmatrix}$$

$$K_3 = \begin{pmatrix} 0 & 0 & 0 & 0 \\ \left(\frac{2}{3}A_1S_0 - 2A_2S_0 - jRB_2d_1\right) & -S_0R\left(\frac{1}{\gamma}+\frac{j}{3R}\right) & j\frac{S_0}{3} & 0 \\ 0 & 0 & 0 & 0 \\ -jRB_3d_1 & 0 & 0 & 0 \end{pmatrix}$$

$$K_4 = \begin{pmatrix} 0 & -j & 0 & 0 \\ Rd_1(1 - jB_7) - jS_0^2 & -2jA_2 & jRB_6 d_1 & 0 \\ 0 & 0 & 0 & -j \\ -jRB_5 d_1 & 0 & Rd_1(1 - jB_8) - jS_0^2 & -2jA_2 \end{pmatrix}$$

Here the following abbreviations have been used:

$$k_0 = \frac{\omega}{C_0} \qquad C_0 = \sqrt{\gamma \mu \bar{T}}_{z=z_0}$$

$$S_0 = \frac{\sqrt{k_x^2 + k_y^2}}{k_0} \qquad C = \sqrt{\gamma \mu \bar{T}(z)}$$

$$A = \frac{1}{2k_0 H} \qquad H = \frac{\mu \bar{T}}{g} = -\frac{\bar{p}}{\bar{p}'}$$

$$A_1 = \frac{1}{2k_0 H_1} \qquad H_1 = -\frac{\bar{\rho}}{\bar{\rho}'}$$

$$A_2 = \frac{1}{2k_0 H_2} \qquad H_2 = -\frac{\eta}{\eta'}$$

$$G = \frac{AC_0}{V} \qquad V = \frac{\kappa g}{c_p \bar{p}}$$

$$d_1 = \frac{C_0^2}{C^2} \qquad d_2 = \frac{\gamma}{(\gamma - 1)}$$

$$\gamma = \frac{c_p}{c_v} \qquad R = \frac{\bar{p}\gamma}{\omega \eta}$$

$$\delta = \frac{1}{1 - \frac{3}{4}\frac{jR}{\gamma}}; \quad Z_1 = \frac{2\Omega}{\omega}; \quad Z_2 = \frac{\nu}{\omega}$$

$$D = 1 + \frac{3}{4}\frac{RZ_2}{\gamma}\cos^2 I + \frac{1}{d_1\gamma}\left(\frac{3}{4}S_0^2 - 4A_1^2 + 4A_1A_2 - \frac{2A_1'}{k_0}\right)$$

$$\left.\begin{matrix} B_1 \\ B_2 \end{matrix}\right\} = Z_1 \sin\vartheta \sin\Lambda_0 \pm Z_2 \sin I \cos I \cos\Lambda_0$$

$$\left.\begin{matrix} B_3 \\ B_4 \end{matrix}\right\} = Z_1 \sin\vartheta \cos\Lambda_0 \pm Z_2 \sin I \cos I \sin\Lambda_0$$

$$\left.\begin{matrix} B_5 \\ B_6 \end{matrix}\right\} = Z_1 \cos\vartheta \pm Z_2 \cos^2 I \cos\Lambda_0 \sin\Lambda_0$$

$$\left.\begin{matrix} B_7 \\ B_8 \end{matrix}\right\} = Z_2 \left(1 - \cos^2 I \left\{\begin{matrix} \cos^2\Lambda_0 \\ \sin^2\Lambda_0 \end{matrix}\right\}\right)$$

$$\cos I = \frac{\sin\vartheta}{\sqrt{1 + 3\cos^2\vartheta}}; \quad \sin I = \frac{2\cos\vartheta}{\sqrt{1 + 3\cos^2\vartheta}}$$

ϑ geographical co-latitude

I geomagnetic dipangle

Λ_0 azimuth

In this calculation the geomagnetic field has been approximated by a dipole field with its axis parallel to the earth's rotational axis. Moreover, the derivative

of μ with respect to z has been neglected. But we have allowed for an altitude dependence of $\bar{\rho}$, $\bar{p}$, η and κ.

For comparison with earlier works (e.g., Hines, 1960; Eckart, 1960) we notice the following characteristic frequencies:

$$\omega_a = \frac{\gamma g}{2C} = \sqrt{d_1}\, A\, \omega$$

$$\omega_g = \frac{2\sqrt{\gamma - 1}}{\gamma}\, \omega_a \qquad \text{(Brunt-Väisälä Frequency)} \qquad (11)$$

$$\omega_h = \frac{\gamma g}{2V} = d_1\, G\, \omega$$

Frequency ω_a is the critical frequency of gravity waves in a loss free isothermal atmosphere. ω_g is a stability parameter for small scale dynamics. ω_h is a measure of the dissipation of wave energy due to heat conduction. The parameter V in ω_h has the dimension of a velocity and can be interpreted as the velocity of vertical heat transport within a static atmosphere in which the ratio $\kappa/\bar{p}$ remains constant (Volland, 1967).

The parameters R and G are proportional to each other:

$$R = \frac{2f}{\gamma} G \qquad (12)$$

with

$$f = \frac{\kappa}{\eta c_v} \sim 2.5$$

(Chapman and Cowling, 1959), indicating the inherent relationship between heat conduction and viscosity. R can be interpreted as some kind of Reynolds number because for acoustic waves the ratio between acceleration force and viscosity force in the equation of momentum is

$$\left| \frac{\rho \frac{\partial \vec{v}}{\partial t}}{\eta \Delta \vec{v}} \right| \sim \frac{\bar{\rho}\omega}{\eta k_0^2} = R$$

If we take into account a mean horizontal velocity of the air with components $(\bar{u}, \bar{v})$ then we only have to replace angular frequency ω by an effective frequency

$$\omega_{eff} = \omega - k_0 S_0 \tilde{\bar{u}}$$

where $\tilde{\bar{u}}$ is the component of mean velocity in the Λ_0-direction of wave propagation as can be derived from Equation (7).

III. THE CHARACTERISTIC WAVES

In order to solve Equation (9) uniquely it is necessary to know the conditions at the lower or the upper boundary of the model atmosphere. Physically appropriate solutions require separation between waves transporting energy upward and waves transporting energy downward. Such waves are the characteristic waves or wave modes. We find them by transforming the matrix of the physical parameters $\mathbf{e}$ in Equation (9)

$$\mathbf{e} = \mathbf{P}\,\mathbf{c} \tag{13}$$

where the column matrix

$$\mathbf{c} = \begin{pmatrix} a_1 \\ \cdot \\ \cdot \\ a_4 \\ b_1 \\ \cdot \\ \cdot \\ b_4 \end{pmatrix} \tag{14}$$

contains four upgoing waves a_i and four downgoing waves b_i. Introducing Equation (13) into Equation (9) gives

$$\mathbf{c}' = j k_0 \mathbf{N}\mathbf{c} - \mathbf{P}^{-1}\mathbf{P}'\,\mathbf{c} \tag{15}$$

$\mathbf{P}$ in Equation (13) has to be chosen in such a manner that the matrix

$$\mathbf{N} = \mathbf{P}^{-1}\mathbf{K}\mathbf{P} = \begin{pmatrix} -\lambda_1 & 0 & \cdots & 0 \\ 0 & & & \vdots \\ \vdots & & -\lambda_i & \vdots \\ 0 & \cdots & 0 & -\lambda_8 \end{pmatrix} \tag{16}$$

in Equation (15) is a diagonal matrix. The elements λ_i in $\mathbf{N}$ are the eigenvalues of $\mathbf{K}$ defined by the eigenvalue equation

$$\left| \mathbf{K} + \lambda_i \mathbf{E} \right| = 0 \tag{17}$$

($\mathbf{E}$ unit matrix).

Within a homogeneous medium in which the elements of $\mathbf{K}$ and $\mathbf{P}$ are constant the characteristic waves now have the solutions

$$\left.\begin{matrix} a_i \\ b_i \end{matrix}\right\} = c_{0i}\, e^{-jk_0 \lambda_i (z - z_0)} \tag{18}$$

and are independent of each other. However, the parameters G, R and Z_2 in $\mathbf{K}$ are altitude dependent even within an isothermal atmosphere. The atmosphere therefore behaves like an inhomogeneous medium with respect to neutral air waves. The matrices $\mathbf{K}$ and $\mathbf{P}$ are functions of height. The matrix $\mathbf{P}^{-1}\mathbf{P}'$ in Equation (15) therefore couples the different characteristic waves with each other at any height.

If this coupling is weak, such that the elements of $\mathbf{P}^{-1}\mathbf{P}'$ are small compared with λ_i, an approximate solution of Equation (15) is

$$\mathbf{c} \sim \mathbf{c}_0\, e^{jk_0 \int_{z_0}^{z} \mathbf{N}(\xi)\, d\xi}$$

or

$$\left.\begin{matrix} a_i \\ b_i \end{matrix}\right\} \sim c_{0i}\, e^{-jk_0 \int_{z_0}^{z} \lambda_i(\xi)\, d\xi} \tag{19}$$

This is the ray solution of Equation (9) (e.g., Budden, 1961). It means that the characteristic waves propagate uncoupled from each other through the inhomogeneous atmosphere and that their amplitude and phase behavior is governed only by their eigenvalues λ_i in the phase integral.

The WKB solution as a second order approximation is defined by a special normalization of the elements of $\mathbf{P}$ such that the matrix $\mathbf{P}^{-1}\mathbf{P}'$ has only zero elements in its diagonal. As a consequence the amplitude factors c_{0i} in Equation (19) become height dependent.

It can be shown by a numerical full wave treatment of Equation (9) that Equation (19) is in fact an excellent approximation at least for ascending gravity waves in thermospheric heights (Volland, 1968).

IV. THE ISOTHERMAL MODEL ATMOSPHERE

In view of the important role of the eigenvalues in any wave treatment our main task in this paper is to find analytical and numerical solutions of the eigenvalue Equation (17). Special analytical solutions have the advantage that they allow a qualitative discussion of the behavior of the characteristic waves and that they help to identify the various wave modes in numerical treatments of the eigenvalue problem.

For convenience we confine ourselves to an isothermal atmosphere. This has the advantage that it substantially simplifies the eigenvalue Equation (17). Moreover it leads to the classical formula of Hines (1960) for an adiabatic atmosphere ($\kappa = \eta = \nu = 0$). This assumption is not really a restriction because in numerical full wave treatments one generally approximates the realistic atmosphere by a number of isothermal slabs (e.g., Midgley and Liehmon, 1966; Volland, 1968). A thickness of 1 km per slab is in most cases a sufficient approximation. In a ray treatment like Equation (19) a change in temperature can be taken into account by a height dependent parameter $A(z)$.

A characteristic wave defined in the foregoing section is completely uncoupled from the other characteristic waves within one slab if the parameters of the coefficient matrix **K** are constant [see Equation (18)]. Then coupling takes place only at the boundaries to the adjacent slabs which have other parameters. If the slab is isothermal with exponentially decreasing pressure and density it follows from the definitions of G, R and Z_2 that the ratios

$$\frac{\kappa}{\bar{p}}, \frac{\eta}{\bar{p}} \text{ and } \frac{\nu}{\omega}$$

must be kept constant within the slab. This involves a constant collision frequency ν and an exponential decrease of κ and η with height such that

$$A_2 = A_1 = A = \text{const.}$$

$$R = \frac{2f}{\gamma} G = \text{const.}$$

$$d_1 = 1.$$

Our model atmosphere therefore has an altitude dependence of the physical parameters as shown in Figure 1. In order to meet the dynamic boundary condition in hydrodynamics the pressure $\bar{p}(z_n)$ must be continuous at the boundary between two adjacent slabs with different temperatures $\bar{T}_n$ and $\bar{T}_{n+1}$.

A more realistic model of the atmosphere could be found by approximating the real temperature profile within one slab by an exponential law

$$\frac{\bar{T}'_n}{T_n} = \text{const.}$$

This would lead to continuous pressure, density and temperature values at the boundaries and an κ-dependence like $\bar{p}$. It would greatly increase however the difficulties in solving Equation (17) and gives no real improvement in numerical calculations.

The profiles shown in Figure 1 approach realistic atmospheric profiles if the thickness Δz_n of the slabs is sufficiently small. Numerical full wave and

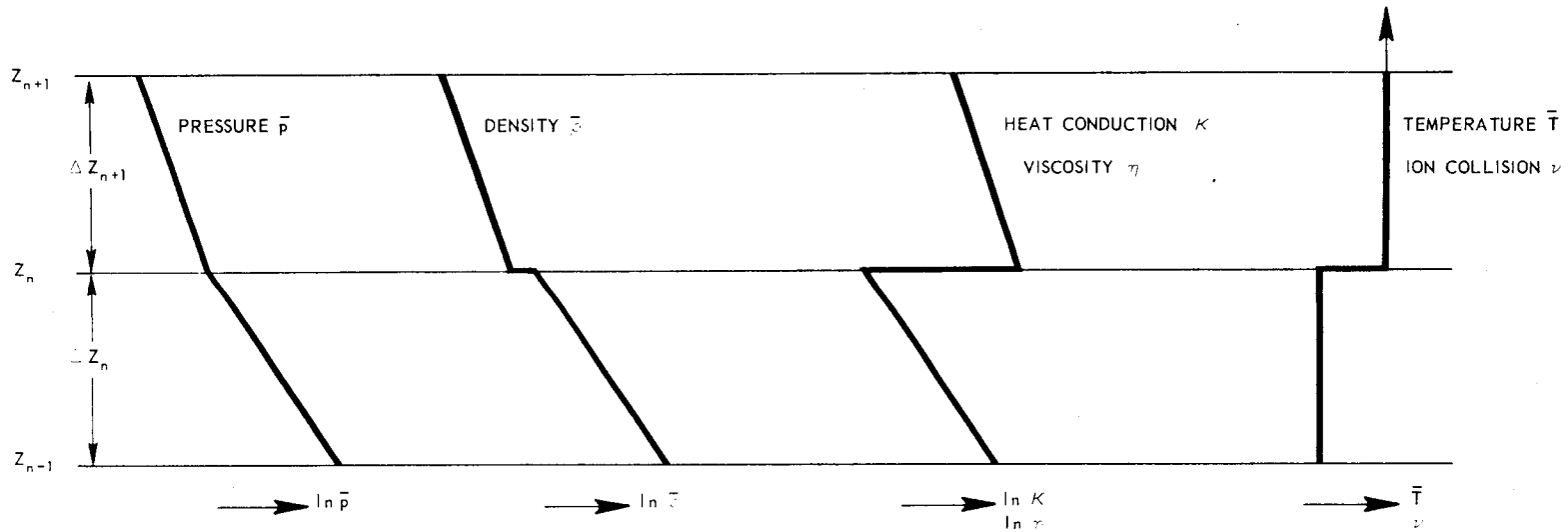

Figure 1. Parameters of the Model Atmosphere in Two Adjacent Isothermal Slabs

ray optics calculations completely justify this kind of approximation including even the strange zigzag profiles of the coefficients of heat conduction κ and viscosity η (Volland, 1968).

V. EIGENVALUES OF AN ISOTHERMAL ATMOSPHERE

From the theory of gravity waves within an isothermal nondissipative atmosphere it is well known (Hines, 1960) that an upgoing wave increases its amplitude like

$$e^{z/2H} \tag{20}$$

in order to keep the wave energy constant in an atmosphere where the pressure decreases exponentially with height. In a dissipative atmosphere the amplitude of a wave cannot surpass the amplitude of the equivalent nondissipative wave because part of the wave energy is transferred into internal energy of the surrounding gas by heat conduction, viscosity or collisions with the plasma component.* We therefore split from the eigenvalue λ_i a positive imaginary part jA:

$$\lambda_i = q_i + jA \tag{21}$$

which describes the amplification of the amplitude as shown in Equation (20).

The remaining term q_1, which we shall refer to as the eigenvalue, is complex:

$$q_i = \alpha_i - j\beta_i \tag{22}$$

Here the real part α_i is a measure of phase velocity V_p:

$$V_p \Big|_i = \frac{C_0}{\sqrt{S_0^2 + \alpha_i^2}} = \frac{C_0}{n_i} \tag{23}$$

(n_i = real refractive index)

*This transfer of energy is a nonlinear process which is not included in our linearized theory.

and of the vertical component of group velocity

$$V_g\Big|_i = \frac{C_0}{\frac{\partial(\omega\alpha_i)}{\partial\omega} - S_0\frac{\partial\alpha_i}{\partial S_0}} \tag{24}$$

The angle between the vertical and the phase velocity is

$$\theta_p\Big|_i = \text{arc tg}\frac{S_0}{\alpha_i} \tag{25}$$

while the angle between the vertical and the direction of the group velocity within the (α_i, S_0) — plane is defined as

$$\theta_g\Big|_i = -\text{arc tg}\frac{\partial\alpha_i}{\partial S_0} \tag{26}$$

The imaginary part $-j\beta_i$ is responsible for the dissipation of wave energy. We define as upgoing or downgoing waves

$$\begin{aligned} \beta_i &\geqq 0 \quad \text{(upgoing)} \\ \beta_i &\leqq 0 \quad \text{(downgoing)} \end{aligned} \tag{27}$$

where the equal signs only stand for nondissipative waves ($\kappa = \eta = \nu = 0$).

VI. CLASSIFICATION OF THE CHARACTERISTIC WAVES IN AN ISOTHERMAL ATMOSPHERE

In this section we shall solve the eigenvalue Equation (17) analytically for some very special cases in an isothermal atmosphere. We shall define the different characteristic waves — or wave modes. As follows immediately from the kind and number of the system of differential Equations (9) there exist four pairs of wave modes, each pair consisting of an upgoing

and a downgoing wave. These four wave pairs are

Acoustic-gravity waves (q_1, q_2)

Heat conduction waves (q_3, q_4)

Ordinary viscosity waves (q_5, q_6)

Extraordinary viscosity waves (q_7, q_8)

In general all eight eigenvalues q_i are different from each other showing that waves belonging to one pair may have different propagation characteristics. In our special analytical solutions we shall find pairs of eigenvalues which only differ in sign (e.g., $q_1 = -q_2$, etc.).

a. Extraordinary Viscosity Waves

We start with the extraordinary viscosity mode because this mode can be easily separated from the other modes. From the eigenvalue Equation (17) it can be seen that this wave mode is coupled with the other waves only through Coriolis force and (or) ion collisions. If Z_1, Z_2 are small compared with 1 the parameters B_n in $\mathbf{K}$ are small and can be neglected. Then the eigenvalue Equation (17) has the form

$$\begin{vmatrix} \mathbf{K}_5 + \lambda_i \mathbf{E} & 0 \\ 0 & \mathbf{K}_6 + \lambda_i \mathbf{E} \end{vmatrix} = 0 \qquad (28)$$

with

$$\mathbf{K}_5 + \lambda_i \mathbf{E} = \left(\begin{array}{cccc:cc} & & & & S_0 & 0 \\ & \mathbf{K}_1 + \lambda_i \mathbf{E} & & & \delta A S_0 j & \frac{-3}{4} S_0 \delta j \\ & & & & 0 & 0 \\ & & & & 0 & 0 \\ \hdashline 0 & 0 & 0 & 0 & \lambda_i & -j \\ \frac{-4}{3} A S_0 & -S_0\left(\frac{R}{\gamma} + \frac{j}{3}\right) & j\frac{S_0}{3} & 0 & R - j S_0^2 & \lambda_i - 2 j A \end{array}\right) \qquad (29)$$

and

$$\mathbf{K}_6 + \lambda_i \mathbf{E} = \begin{pmatrix} \lambda_i & -j \\ R - j S_0^2 & \lambda_i - 2jA \end{pmatrix} \tag{30}$$

Now the eigenvalue equation can be separated into two determinants:

$$|\mathbf{K}_5 + \lambda_i \mathbf{E}| \cdot |\mathbf{K}_6 + \lambda_i \mathbf{E}| = 0$$

which implies:

$$|\mathbf{K}_5 + \lambda_i \mathbf{E}| = 0 \tag{31}$$

$$|\mathbf{K}_6 + \lambda_i \mathbf{E}| = 0 \tag{32}$$

The solution of Equation (32) is

$$\lambda_{\substack{7\\8}} - jA = q_{\substack{7\\8}} = \mp j\sqrt{A^2 + S_0^2 + jR} \tag{33}$$

$$(Z_1 = Z_2 = 0)$$

$q_{\substack{7\\8}}$ are the eigenvalues of the pair of extraordinary viscosity waves. The upper sign in Equation (33) stands for the ascending wave, the lower sign stands for the descending wave as one can check immediately from the definitions given in Equations (27). This wave mode is a purely transverse wave inasmuch as only the horizontal component $\Delta\tilde{v}$ orthogonal to the direction of wave propagation is involved. It is heavily attenuated for large values of R and becomes a purely evanescent wave at R = 0.

Equation (33) is also exact for east-west propagation ($\Lambda_0 = \pm 90°$) at the equator ($\vartheta = 90°$) even for arbitrary values of Z_1 and Z_2. In this case the wave is likewise completely uncoupled from the other waves.

From Equations (23) and (24) we derive phase and group velocity at vertical incidence as

$$V_p \sim \begin{cases} \pm \dfrac{2C_0 A}{R} & \text{for } A >> R \\ \pm \dfrac{C_0\sqrt{2}}{\sqrt{R}} & \text{for } A << R \end{cases} \qquad (34)$$

$$V_g \sim \begin{cases} V_p & \text{for } A >> R \\ 2V_p & \text{for } A << R \end{cases}$$

Phase and group velocity have the same direction.

b. Ordinary Viscosity Waves

The remaining Equation (31) can similarly be separated for vertical incidence $S_0 = 0$. Then Equation (31) becomes

$$\left| \mathbf{K}_5 + \lambda_i \mathbf{E} \right| = \begin{vmatrix} \mathbf{K}_1 + \lambda_i \mathbf{E} & 0 \\ 0 & \mathbf{K}_7 + \lambda_i \mathbf{E} \end{vmatrix} = 0 \qquad (35)$$

$\mathbf{K}_7$ looks exactly like $\mathbf{K}_6$ in Equation (32) for $S_0 = 0$ and gives the eigenvalues of the pair of ordinary viscosity waves

$$q_{\substack{5 \\ 6}} = \mp j\sqrt{A^2 + jR} \qquad (36)$$

$$(S_0 = Z_1 = Z_2 = 0)$$

which have the same behavior as the eigenvalues of the extraordinary viscosity waves.

c. Acoustic-Gravity Waves and Heat Conduction Waves

The eigenvalues of the remaining matrix K_1 in Equation (35) can be found for $S_0 = 0$ as

$$\left.\begin{matrix} q_{\frac{1}{2}} \\ \\ q_{\frac{3}{4}} \end{matrix}\right\} = \mp j\sqrt{A^2 + \frac{j}{\gamma}(G + R^*) \mp \frac{j}{\gamma}\sqrt{(G + R^*) - \frac{4GR^*}{1 - \frac{2jG}{\gamma d_2}}}} \qquad (37)$$

$$(S_0 = Z_1 = Z_2 = 0)$$

with

$$R^* = \frac{j\gamma}{2}(1 - \delta)\left(\gamma - \frac{2jG}{d_2}\right) \sim \begin{cases} \frac{3}{8}\gamma R & R << 1 \\ \text{for} & \\ \frac{(\gamma - 1)\gamma}{2f} R & R >> 1 \end{cases}$$

The negative sign within the square root in Equation (37) is related to acoustic-gravity waves, the positive sign is related to heat conduction waves. The signs outside the square root are again due to ascending and descending waves.

Approximate solutions of Equation (37) are

$$\left.\begin{matrix} q_{\frac{1}{2}} \\ \\ q_{\frac{3}{4}} \end{matrix}\right\} \sim \begin{cases} \mp j\sqrt{A^2 + \frac{3}{4} jR} & \\ & \text{for } G, R << 1 \\ \mp j\sqrt{A^2 + \frac{2jG}{\gamma}} & \end{cases}$$

$$\left.\begin{matrix} q_1 \\ q_2 \end{matrix}\right\} \sim \begin{cases} \pm\sqrt{1 - A^2} & \\ & \text{for } G, R >> 1 \\ \mp j\sqrt{A^2 + 2jG} & \end{cases} \qquad (38)$$

$$\left.\begin{matrix} q_3 \\ q_4 \end{matrix}\right\}$$

$$(S_0 = Z_1 = Z_2 = 0)$$

Equations (38) indicate as expected that for small Reynolds numbers ($R << 1$) all wave modes including the acoustic-gravity mode are evanescent waves behaving like viscosity waves while for large Reynolds numbers ($R >> 1$) heat conduction waves behave like viscosity waves but acoustic-gravity waves are propagation waves for $A < 1$ (acoustic wave range) and are evanescent waves (at vertical incidence) for $A > 1$ (gravity wave range).

VII. APPROXIMATE SOLUTIONS OF THE EIGENVALUE EQUATION AT LARGE REYNOLDS NUMBERS ($\eta \to 0$)

An important approximation of the general eigenvalue Equation (17) can be found if one makes the assumption

$$R >> \begin{cases} A \\ S^2 \end{cases} \qquad (39)$$

In this case we again can split the determinant $|\mathbf{K} + \lambda_i \mathbf{E}|$ into two nearly independent determinants:

$$|\mathbf{K} + \lambda_i \mathbf{E}| \sim \begin{vmatrix} \bar{\mathbf{K}}_1 + \lambda_i \mathbf{E} & 0 \\ 0 & \mathbf{K}_4 + \lambda_i \mathbf{E} \end{vmatrix} = 0 \qquad (40)$$

We do this by multiplying the 5th and the 7th column of $|\mathbf{K} + \lambda_i \mathbf{E}|$ with factors h_1 and h_2, respectively, and add both columns to the first column. We next multiply the 5th and 7th column by

$$\frac{S_0}{\gamma} h_3 \text{ and } \frac{S_0}{\gamma} h_4$$

and add both columns to the second column. Here it is

$$\begin{aligned} h_1 &= (B_3 B_6 + B_2 B_8 + j B_2)/\Delta \\ h_2 &= (B_3 B_7 - B_2 B_5 + j B_3)/\Delta \\ h_3 &= (1 - j B_8)/\Delta \\ h_4 &= j B_5/\Delta \\ \Delta &= 1 - B_5 B_6 - B_7 B_8 - j(B_7 + B_8) \end{aligned} \tag{41}$$

This procedure eliminates the R dependence of the off diagonal submatrices in Equation (17), since $\delta \to 0$ and

$$R\delta \to \frac{4j}{3\gamma}.$$

Their elements therefore become negligibly small compared with the elements of the submatrix $\mathbf{K}_4 + \lambda_i \mathbf{E}$ if R goes to infinity. Thus the eigenvalues of the viscosity waves can be determined from the determinant

$$|\mathbf{K}_4 + \lambda_i \mathbf{E}| = 0$$

as

$$\left.\begin{matrix} q_5 \\ 6 \\ \\ \\ q_7 \\ 8 \end{matrix}\right\} \sim \mp j\sqrt{A^2 + S_0^2 + \frac{R}{2}(B_7 + B_8) + jR \pm jR\sqrt{B_5 B_6 - \frac{1}{4}(B_7 - B_8)^2}} \tag{42}$$

The remaining determinant in Equation (40) has the form

$$|\bar{K}_1 + \lambda_i E| = \begin{vmatrix} \lambda_i + h_1 S_0 - 2jA & -\left(1 - \frac{h_3 S_0^2}{\gamma}\right) & 1 & 0 \\ -\gamma(1 - h_5) & \lambda_i - h_6 S_0 & -2jA & \frac{4}{3}\gamma\frac{(\gamma - 1)}{f} \\ 0 & 0 & \lambda_i & -\frac{2jG}{d_2} \\ -2jA & -1 & d_2\left(1 + \frac{S_0^2}{2jG}\right) & \lambda_i - 2jA \end{vmatrix} = 0 \tag{43}$$

with

$$h_5 = j(Z_2 \cos^2 I - B_1 h_1 - B_4 h_2)$$

$$h_6 = j(B_1 h_3 + B_4 h_4)$$

It can be shown that the element

$$K_{24} = \frac{4}{3}\gamma\frac{(\gamma - 1)}{f} \sim 0.4$$

which is the only direct contribution of R via the parameter δ in this determinant can entirely be neglected as long as

$$A >> K_{24} .$$

This is in the gravity wave range.

The negligence of the term K_{24} in Equation (43) means that we treat the system of Equations (2) without taking into account viscosity ($\eta = 0$). The transformation of the determinant Equation (40) has then the effect of eliminating the horizontal components of the velocity in the momentum Equations (2) which are coupled via Coriolis force and (or) ion drag with the vertical component of the velocity Δw and with the pressure Δp. The terms h_1 and h_6 in Equation (43) are now contributions of the vertical wind velocity and of the horizontal pressure gradient. They are of the order $\lesssim 1$ and therefore small compared with A or $|\lambda_i|$.

If we neglect in Equation (43) the element K_{24} and all terms which include the difference $h_1 - h_6$, the solution of Equation (43) becomes

$$\left.\begin{matrix} q_1 \\ 2 \\ \\ \\ q_3 \\ 4 \end{matrix}\right\} \sim \mp j\sqrt{A^2 + S_0^2 - \frac{h_7}{2} + jG \pm \sqrt{\left(\frac{h_7}{2} - jG\right)^2 + 2jG(h_8 + S_0^2 B^2 h_3)}} \qquad (44)$$

$$(\eta = 0;\ h_1 - h_6 \sim 0)$$

with

$$h_7 = S_0^2(1 + h_1 h_6) + (1 - h_5)(\gamma - S_0^2 h_3) - j S_0 A(h_1 + h_6)$$

$$h_8 = h_7 - (\gamma - 1)(1 - h_5) + \frac{2j S_0 A}{d_2}(h_1 + h_6)$$

$$B^2 = \frac{4A^2}{d_2 \gamma} = \frac{\omega_g^2}{\omega^2}$$

Again the upper sign within the square root is for acoustic-gravity waves, the lower sign is for heat conduction waves.

For east-west propagation ($\Lambda_0 = \pm 90°$) at the equator ($\vartheta = 90°$) it is $h_1 = h_6$, and Equation (44) is exact provided $K_{24} = 0$.

For $Z_1 = Z_2 = 0$ it is

$$h_7 = \gamma$$

$$h_8 = h_3 = 1$$

$$h_1 = h_2 = h_4 = h_5 = h_6 = 0$$

Then Equation (44) becomes identical with Pitteway and Hines (1963) Equation (36).

From our assumption made in Equation (39) we should expect that the approximate Equation (44) breaks down for small values of R (and therefore of G). Surprisingly enough we shall find from numerical calculations given in the next section that Equation (44) is a reasonable approximation even for

$$G \gtrsim A \gtrsim 1$$

which is within the range of gravity waves as long as S_0 is not too large.

VIII. NUMERICAL SOLUTIONS OF THE EIGENVALUE EQUATION

Apart from some special analytical solutions which are given in the previous sections, Equation (17) has to be treated by numerical methods. A convenient program available in the SHARE Program Catalog is SAD 3099 (EIG 4) which solves eigenvalues of complex matrices and is coded for the IBM 7090/94. This program has been used for the following calculations.

The atmospheric model used is the Harris-Priester model 5 at 1200 local time in 200 and 400 km height (CIRA, 1965). The parameters of this model together with additional numerical values are given in Table I.

Table I

Numerical Data Used in the Calculations of Eigenvalues

z(Km)	$\omega_a (s^{-1})$	$\omega_h (s^{-1})$	$\nu (s^{-1})$	$\Omega (s^{-1})$	γ	f	C_0 (m/s)	V(m/s)
200	8.93×10^{-3}	1.09	$1. \times 10^{-4}$	7.27×10^{-5}	1.5	2.5	773.0	6.35
400	6.51×10^{-3}	3.92×10^{-2}	$1. \times 10^{-4}$	7.27×10^{-5}	1.5	2.5	999.0	166.0

In each of the following figures the eigenvalues of the different wave modes has been plotted versus the normalized horizontal wave number

$$S_0 = \frac{\sqrt{k_x^2 + k_y^2}}{k_0}.$$

The curve parameter is the angular frequency ω(in sec^{-1}). The left side of each figure gives the real part α_i of the eigenvalue. The right side gives its negative imaginary part multiplied by k_0: $k_0\beta_i$. We restrict ourselves to ascending waves. The eigenvalues of descending waves are not very much different from the eigenvalues of the equivalent ascending waves (apart of course from the sign).

Figures 2-5 show results of numerical claculations of the eigenvalue Equation (17) (full lines). For comparison the dashed lines have been calculated from the approximate formula Equation (44) with the same numerical data. The propagation conditions in these calculations are east to west propagation ($\Lambda_0 = 90°$) at the equator ($\vartheta = 90°$). In order to arrange that the various curves fit within one figure, the ordinate of α_1 in Figures 2 and 6 has been divided into two different scales — a linear one for $\alpha_1 \geq -1$, and a logarithmic one for $\alpha_1 < -1$.

From the definitions of magnitude and direction of phase velocity [Equations (23) and (25)] it follows that the vector from the origin to a point of the dispersion curves gives the ratio between velocity of sound to phase velocity and the direction of phase velocity. We observe in Figure 2 the well known downward directed phase velocity of the ascending gravity waves ($\omega < \omega_a$) while their energy propagation vector defined by Equations (24) and (26) is orthogonal to the dispersion curves of α_i (S_0) and is directed upward.

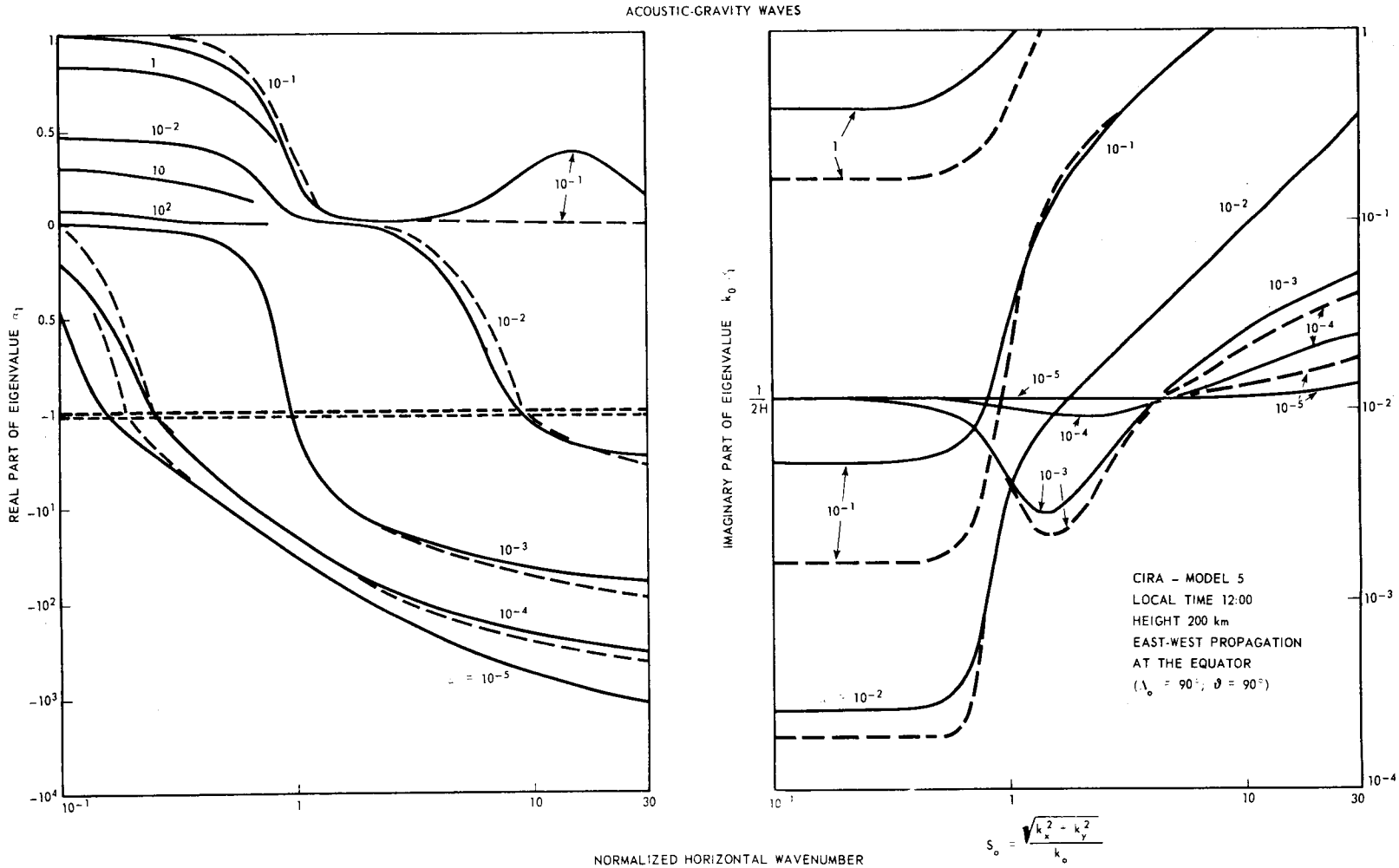

Figure 2. Real part α_1 (left) and negative imaginary part $k_0 \beta_1$ (right) of eigenvalues of ascending acoustic-gravity waves versus normalized horizontal wave number S_0. Parameter is the angular frequency ω (in sec^{-1}). Full lines are calculated from Equation (17) taking into account viscosity, dashed lines are calculated from Equation (44) neglecting viscosity ($\eta = 0$). Propagation conditions: east to west propagation ($\Lambda_0 = 90°$) at the equator ($\vartheta = 90°$) in 200 km height.

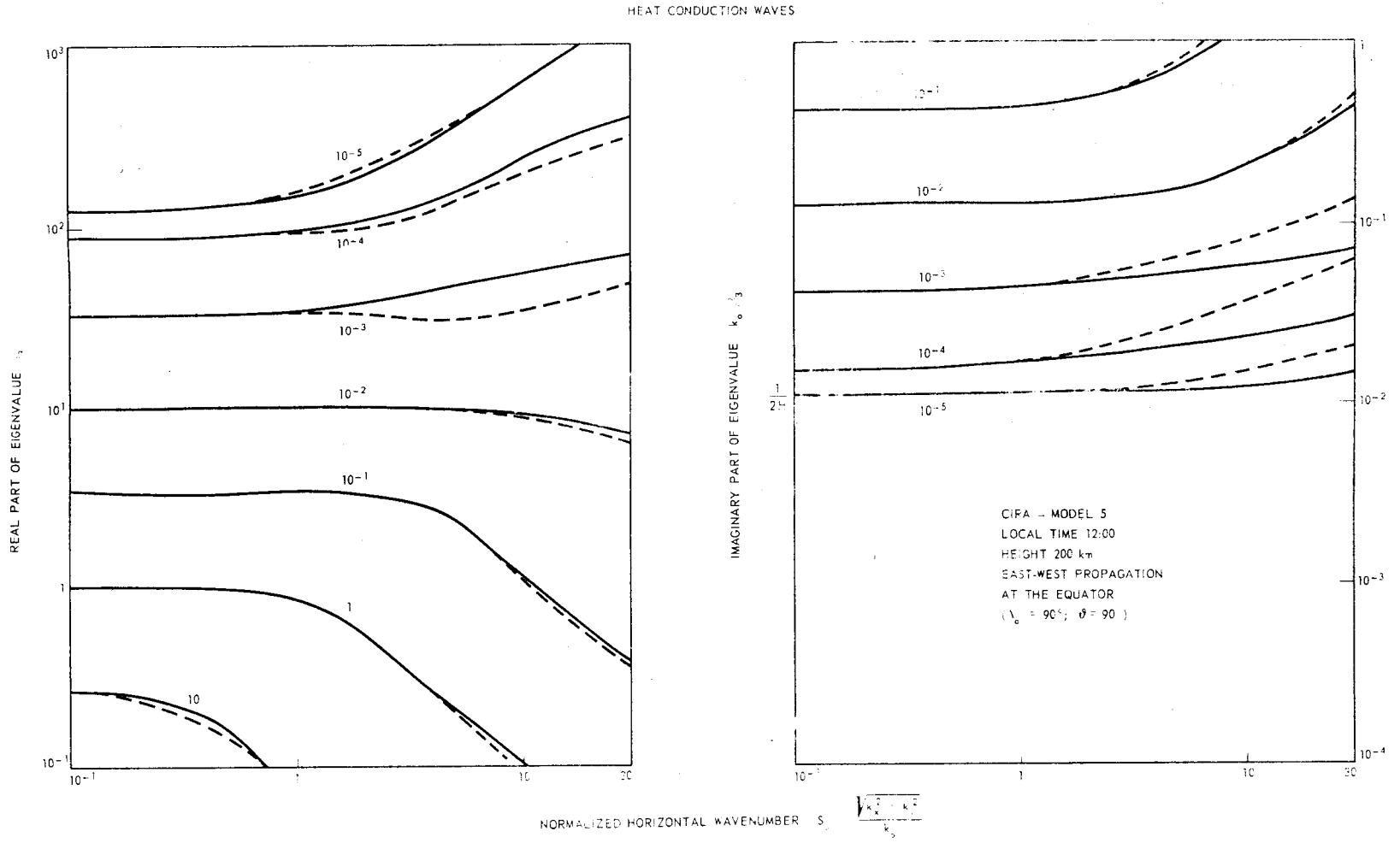

Figure 3. Real part α_3 (left) and negative imaginary part $k_0 \beta_3$ (right) of eigenvalues of ascending heat conduction waves. For details see text of Figure 2.

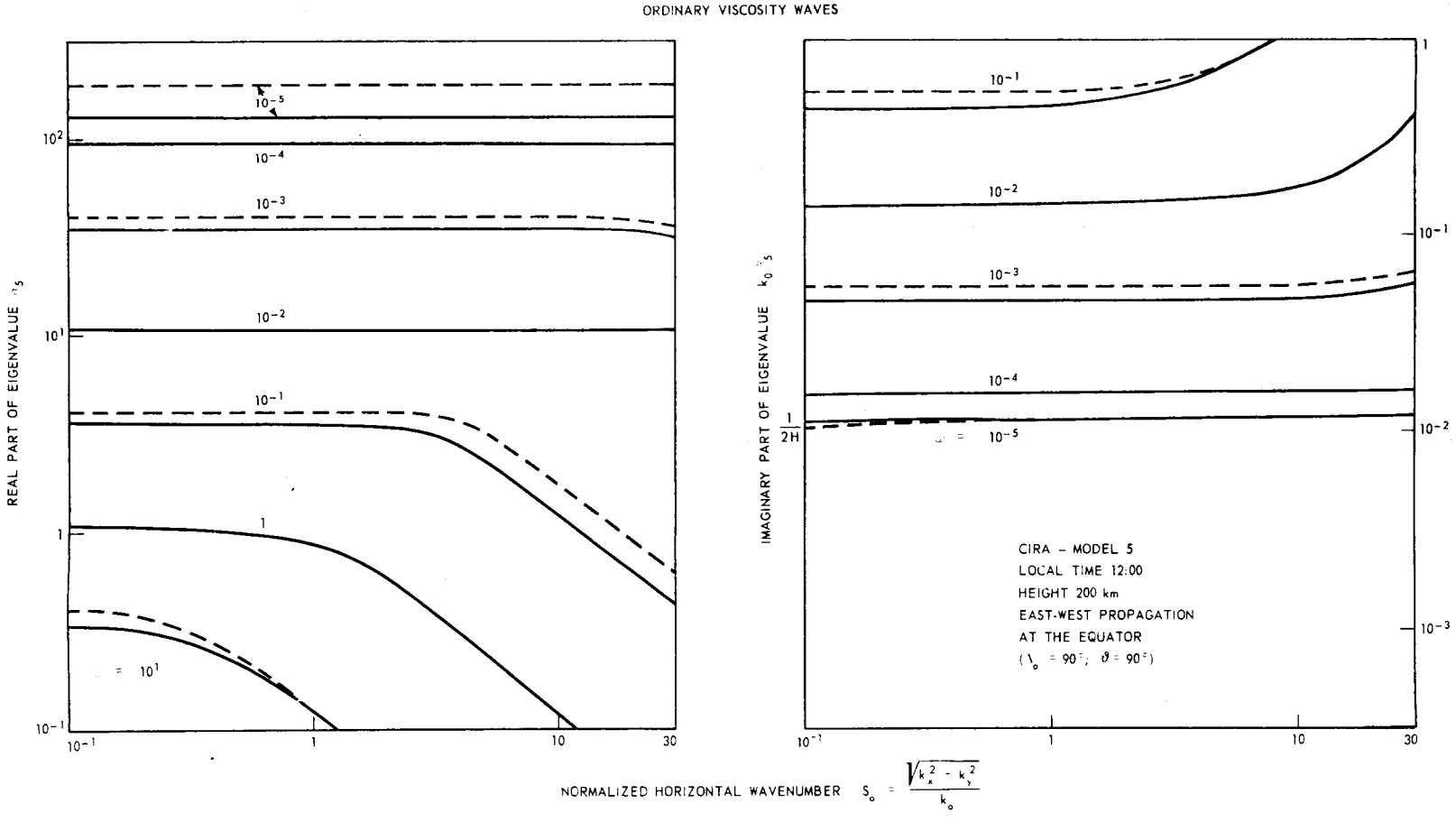

Figure 4. Real part α_5 (left) and negative imaginary part $k_0 \beta_5$ (right) of eigenvalues of ascending ordinary viscosity waves. For details see text of Figure 2.

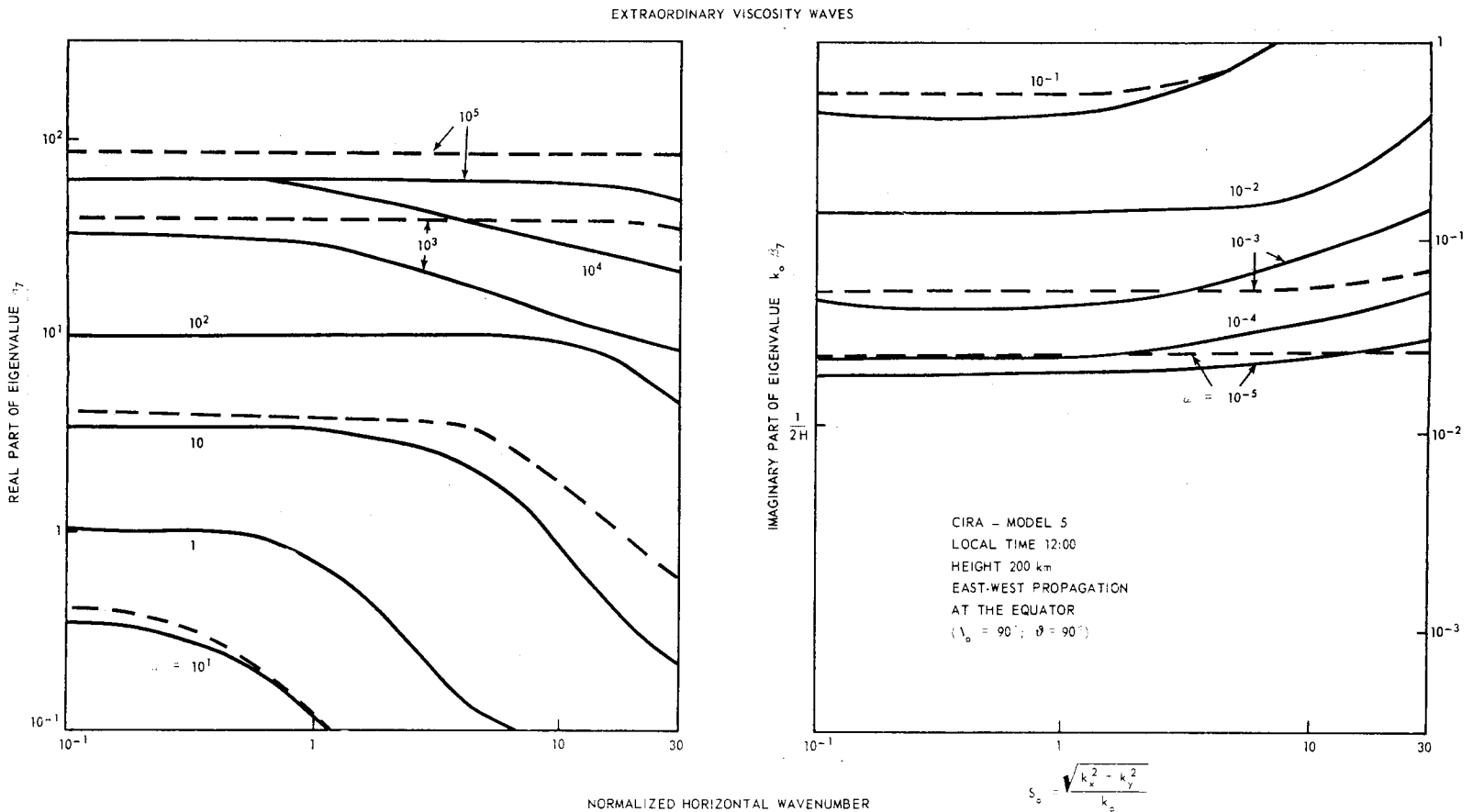

Figure 5. Real part α_7 (left) and negative imaginary part $k_0 \beta_7$ (right) of eigenvalues of ascending extraordinary viscosity waves. For details see text of Figure 2.

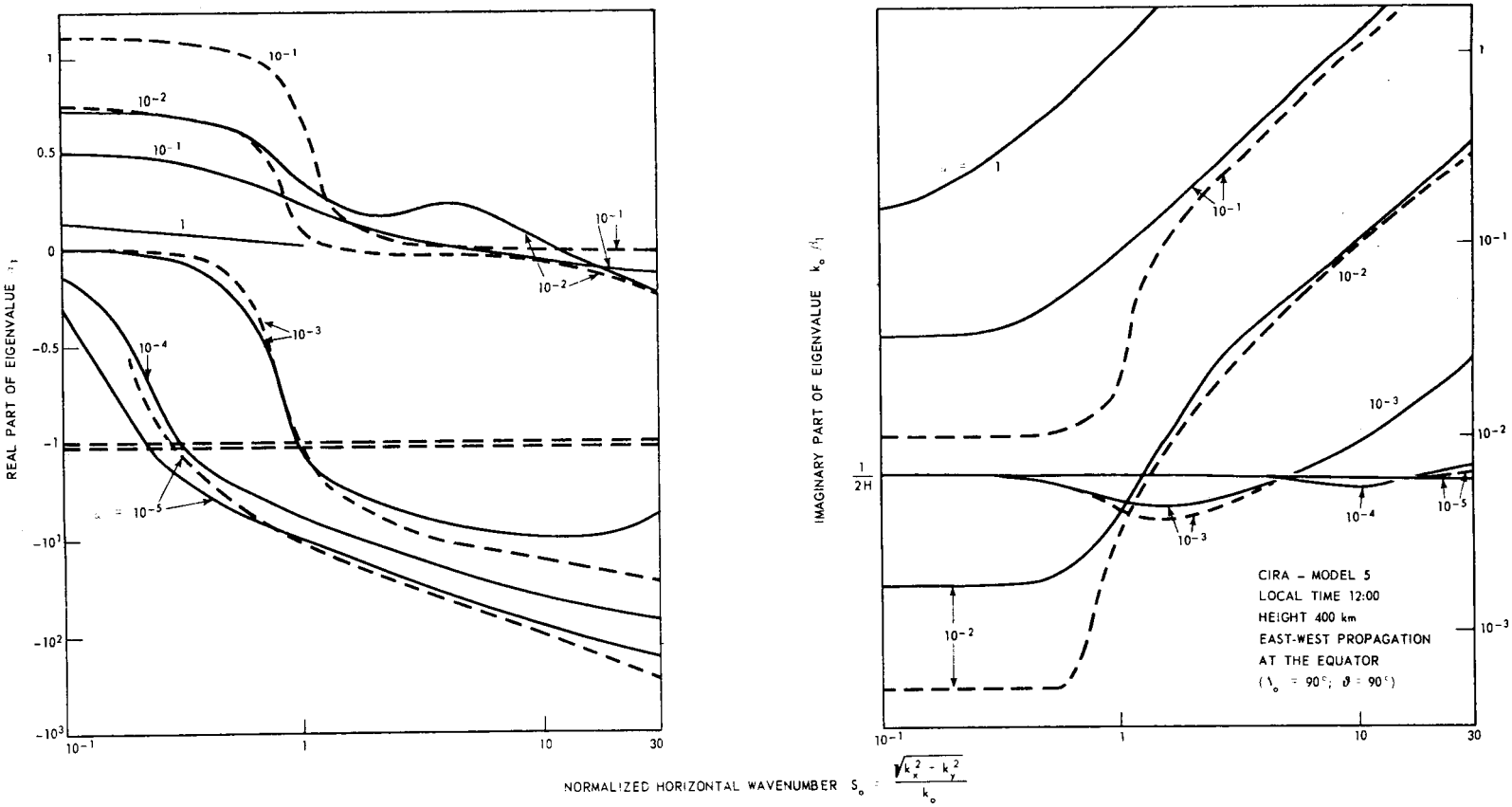

Figure 6. Real part α_1 (left) and negative imaginary part $k_0 \beta_1$ (right) of eigenvalues of ascending acoustic-gravity waves in 400 km height. For further details see text of Figure 2.

Acoustic waves ($\omega > \omega_a$) with Reynolds numbers $R \gtrsim 1$ show a normal behavior, but become evanescent waves at $R < 10^{-1}$ as expected from Equation (38).

The intermittent frequency ($\omega_a \sim \omega = 10^{-2}$ sec^{-1}) shows acoustic wave features at $S_0 < 1$ and gravity wave features at $S_0 > 1$ with a continuous transition region. From Figure 2 (attenuation factors $k_0\beta_1$) it follows however that the gravity wave range of this frequency is heavily attenuated.

From the definition of the attenuation factor [Equations (22) and (27)] we can deduce that the wave amplitude of an upgoing wave remains constant if

$$\beta_i = \frac{1}{2H}$$

This is the general behavior for gravity waves ($\omega < \omega_a$) and $S_0 < 10$ in Figure 2. The frequency $\omega = 10^{-3}$ s^{-1} has a minimum of attenuation at $S_0 = 1.5$. At this frequency and horizontal wave number ($k_y \sim 2 \times 10^{-3}$ km^{-1}) we expect therefore especially good propagation conditions in this altitude range. The atmosphere seems to behave like a frequency and height dependent selective filter with respect to gravity waves.

Acoustic waves with frequencies $\omega > 1$ s^{-1} are heavily damped and do not contribute to energy transport in this height.

The dashed lines in Figure 2 calculated from the approximate formula Equation (44) indicate that this formula is a reasonable approximation within the gravity wave range ($A \gtrsim 1$ or $\omega_a \gtrsim \omega$). It breaks down in the acoustic range. There one expects from Equation (44) a phase velocity

$$V_p \sim \frac{C_0}{\gamma}$$

for $\omega \to \infty$ while Equation (38) predicts $V_p \to 0$.

Figures 3 to 5 show real and imaginary part of eigenvalues of heat conduction wave, ordinary and extraordinary viscosity waves. All three wave modes behave very similar in the whole frequency range. Heat conduction waves are slightly less attenuated than viscosity waves

For $A > 1$ and $S_0 > 10$ real and imaginary part of the eigenvalues in Figures 3 to 5 are of the same order of magnitude as the gravity waves (Figure 2). The sign of α_i in Figures 3 to 5 is always positive at this height indicating that energy and phase normal are equally directed.

Within the acoustic range ($A < 1$) all three wave modes in Figures 3 to 5 tend to become heavily attenuated evanescent modes. ($k_0 \beta_i = 1$ is equivalent to a decrease in amplitude of 1/e after a vertical propagation path of 1 km.) Neither mode ever shows an increase in amplitude with height.

The dashed lines in Figures 3 to 5 have been calculated from Equations (42) and (44) and give evidence of the rather good approximation which these formulae provide.

In order to check the validity of Equation (44) as compared with the exact Equation (17) the calculations have been repeated in Figure 6 for gravity waves using the parameters at a height of 400 km (see Table I) and the same propagation conditions ($\Lambda_0 = 90°$; $\vartheta = 90°$). We observe again a reasonably good agreement between the exact solutions from Equation (17) (full lines) and the approximative solution from Equation (44) (dashed lines) for the gravity wave range ($A > 1$).

This agreement breaks down for $A > G$ or for very large S_0 values. $A \sim G$ holds in about 500 km. Below this height the error arising from Equation (44) seldom exceeds 50% in the gravity wave range. In view of the great simplification given by Equation (44) as compared with the exact expression Equation (17) this error seems to be of an allowed order. However the approximate decoupling of the viscosity waves from the gravity and heat conduction waves greatly simplifies any full wave treatment. It justifies for instance Harris' and Priester's (1962) calculations in which the coefficient of viscosity has been neglected.

In order to investigate the influence of Coriolis force and ion drag we compare in Figures 7 to 10 the real and imaginary part of eigenvalues of gravity waves at 200 km for south to north propagation ($\Lambda_0 = 180°$) with east to west propagation ($\Lambda_0 = 90°$) (dashed lines) at the equator ($\vartheta = 90°$) (Figures 7 and 8) and at 45° northern latitude ($\vartheta = 45°$) (Figures 9 and 10). Moreover we compare these dispersion curves with the eigenvalues of gravity waves where Coriolis force and ion drag have been neglected ($Z_1 = Z_2 = 0$) (full lines). Again the exact expression Equation (17) (Figures 7 and 9) and the approximate solution Equation (44) (Figures 8 and 10) have been used.

From these figures we see that Coriolis force and ion drag makes the atmosphere anisotropical with respect to gravity waves. In Figure 7 the eigenvalues for $Z_1 = Z_2 = 0$ (full lines) are equal to the eigenvalues at south to north

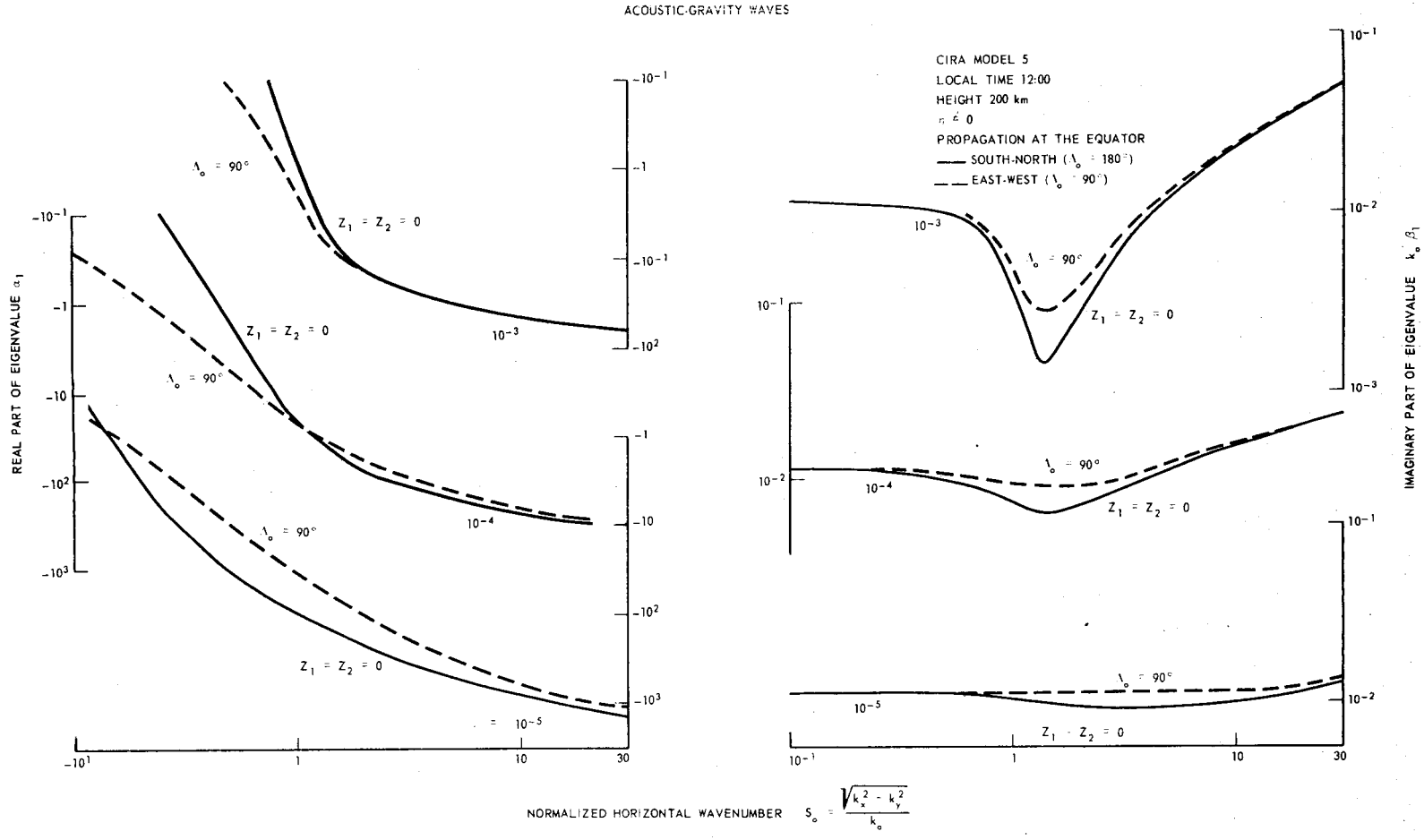

Figure 7. Real part α_1 (left) and negative imaginary part $k_0 \beta_1$ (right) of eigenvalues of ascending gravity waves in 200 km height calculated from Equation (17) taking into account viscosity. Propagation conditions: Equator ($\vartheta = 90°$). Full lines: south to north propagation ($\Lambda_0 = 180°$) and $Z_1 = Z_2 = 0$. Dashed lines: east to west propagation ($\Lambda_0 = 90°$).

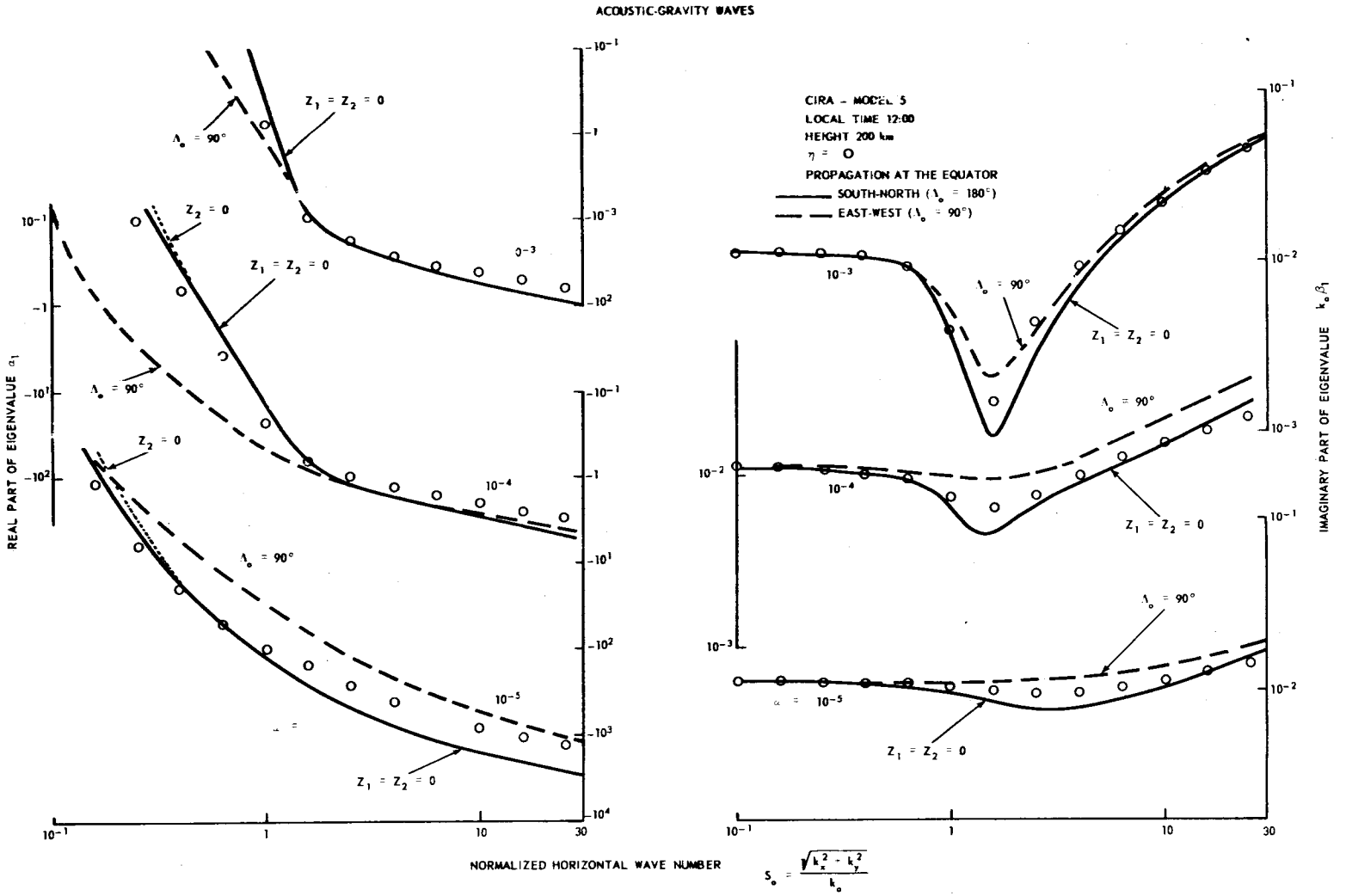

Figure 8. Same as Figure 7, but calculated from Equation (44) neglecting viscosity ($\eta = 0$). Dotted curves are calculated neglecting ion drag ($Z_2 = 0$; $\Lambda_0 = 90°$). Circles are calculated from Equation (17) for $Z_1 = Z_2 = 0$.

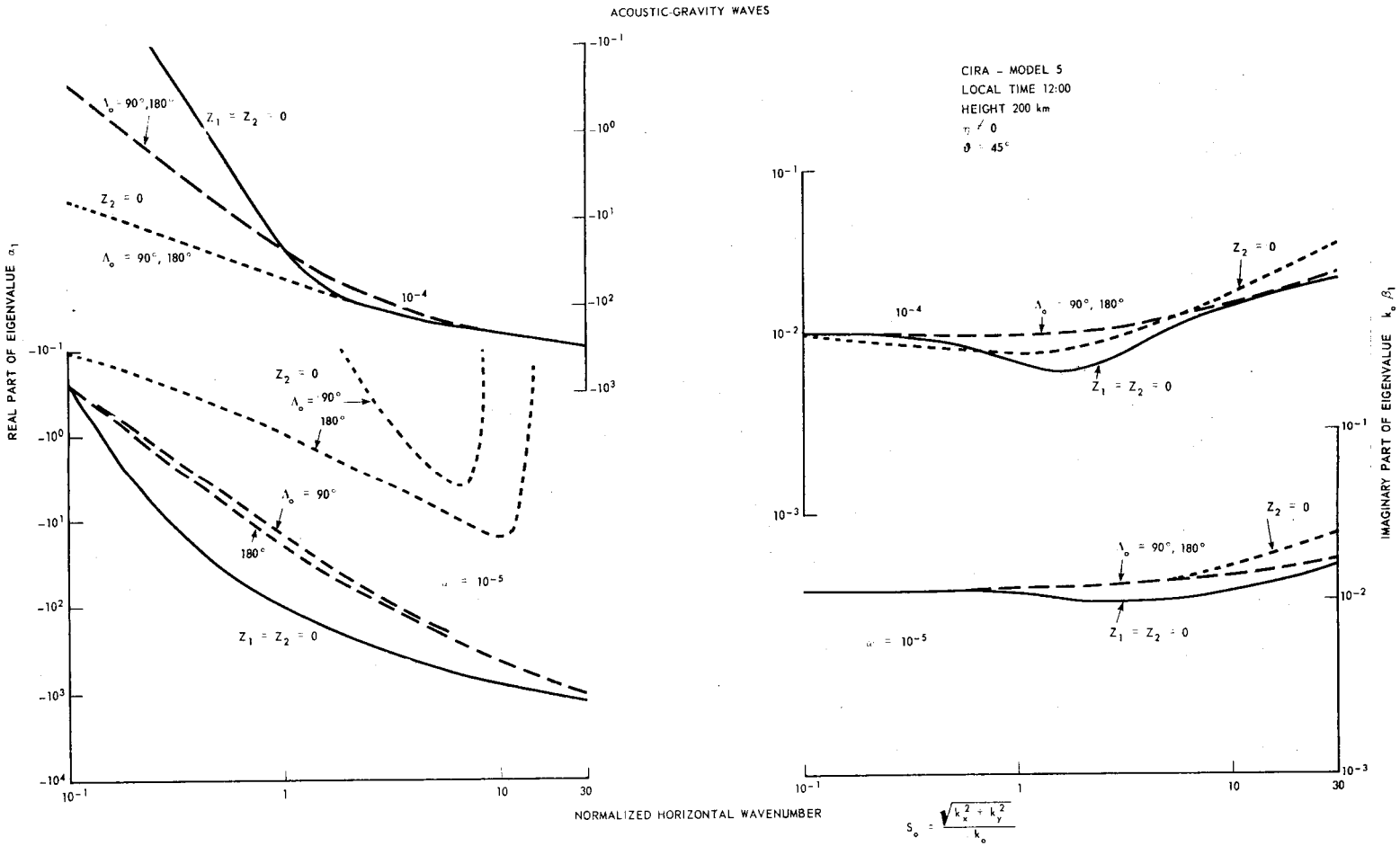

Figure 9. Real part α_1 (left) and negative imaginary part $k_0 \beta_1$ (right) of eigenvalues of ascending gravity waves in 200 km height calculated from Equation (17) taking into account viscosity. Propagation conditions: 45° northern latitude ($\vartheta = 45°$). Full lines: $Z_1 = Z_2 = 0$. Dashed lines: South to north ($\Lambda_0 = 180°$) and east to west ($\Lambda_0 = 90°$) propagation; $Z_1, Z_2 \neq 0$. Dotted lines: South to north ($\Lambda_0 = 180°$) and east to west ($\Lambda_0 = 90°$) propagation; $Z_1 \neq 0$; $Z_2 = 0$.

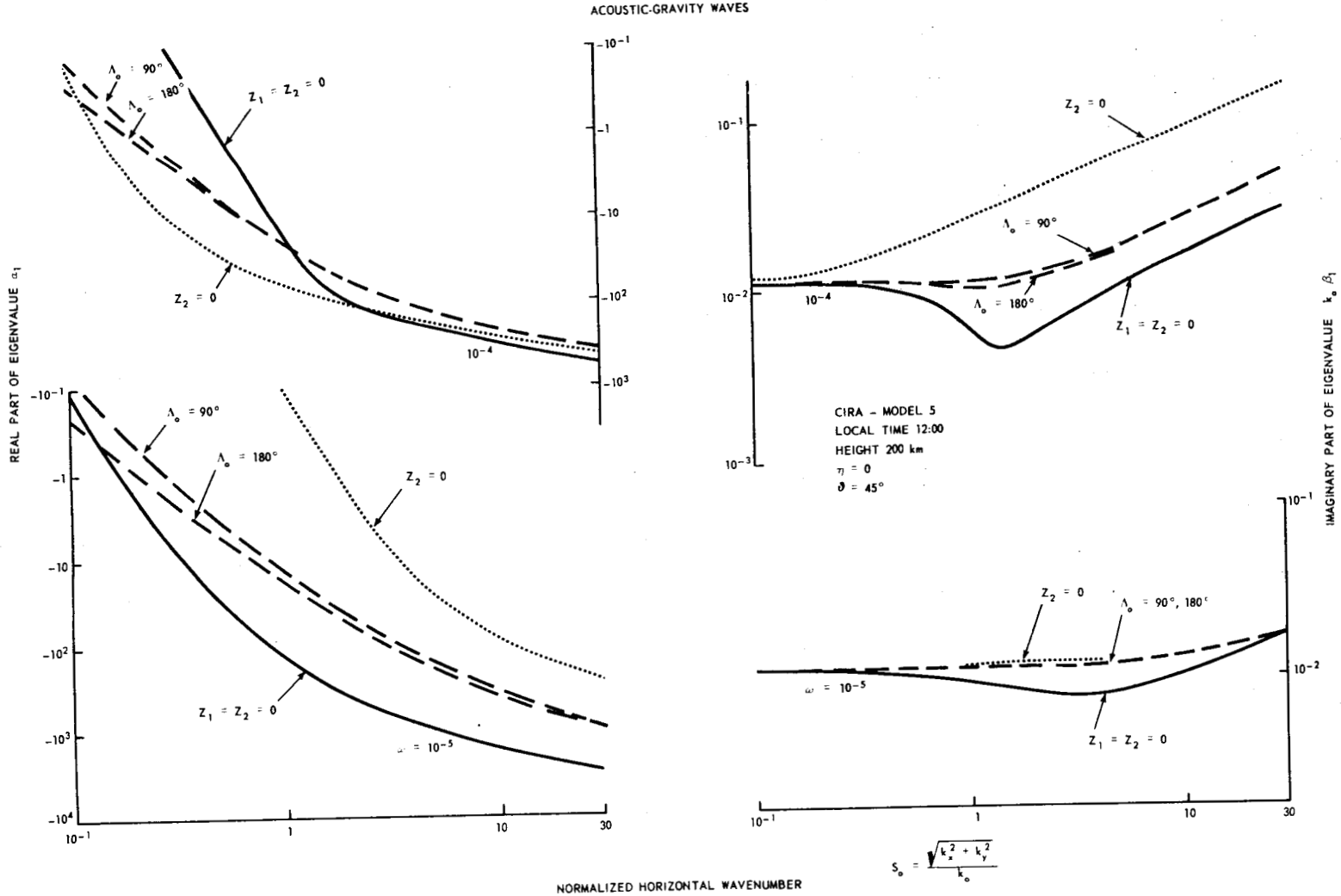

Figure 10. Real part α_1 (left) and negative imaginary part $k_0 \beta_1$ (right) of eigenvalues of ascending gravity waves calculated from Equation (44) neglecting viscosity ($\eta = 0$). For further details see text of Figure 9.

propagation ($\Lambda_0 = 180°$). Coriolis force and ion drag therefore only affect east to west propagation ($\Lambda = 90°$) (dashed lines). The attenuation minimum at $S_0 \sim 1$ becomes deeper for south to north paths as compared with east to west paths suggesting more favorable propagation conditions for south to north paths.

In these and all the following calculations it has been found that for west to east propagation the eigenvalues do not differ more than 10% from the values of east to west propagation. The same is true for north to south paths in relation to south to north paths.

Figure 8 gives the same results as in Figure 7 but calculated from Equation (44) ($\eta = 0$). For comparison the circles are drawn from the full lines in Figure 7 giving the exact calculation for $Z_1 = Z_2 = 0$. The dotted lines have been calculated from the conditions $Z_2 = 0$, $\Lambda_0 = 90°$ indicating small influence of Coriolis force at the equator. From comparing Figures 7 and 8 we again observe a rather good agreement between values calculated from Equations (17) and (44). We note that even special features of the single curves in Figure 7 are truly reflected in Figure 8.

Finally Figures 9 and 10 give results at 45° northern latitude ($\vartheta = 45°$). Here we observe for the first time a remarkable difference between the results from Equations (17) and (44). It arises for the case $\omega = 10^{-5}$ sec^{-1}, negligible ion drag ($Z_2 = 0$) and $S_0 > 6$. Here the exact α_1-curves (dotted curves) bend toward zero and then become positive for increasing S_0 values. The equivalent α_1 curve in Figure 10 (dotted curve) behaves in the normal manner and shows no difference for $\Lambda_0 = 180°$ and $\Lambda_0 = 90°$. It differs however appreciably from the full curve ($Z_1 = Z_2 = 0$) giving evidence of the large influence of Coriolis force on the propagation characteristics in medium latitudes. If we add ion drag which in our calculations is of the same order of magnitude as the Coriolis force we find the dashed curves in Figures 9 and 10. Here ion drag has the tendency to reduce the influence of the Coriolis force.

At $\omega = 10^{-4}$ sec^{-1} the attenuation factor is larger in Figure 10 than in Figure 9 for $Z_2 = 0$. Again ion drag reduces substantially this difference.

IX. CONCLUDING REMARKS

It has been shown that eight obliquely incident plane characteristic waves can propagate through a horizontally stratified atmosphere, four of them

ascending and the other four descending. The four pairs of characteristic waves are the well known acoustic-gravity waves, the heat conduction waves and ordinary and extraordinary viscosity waves. Heat conduction waves and viscosity waves are named according to their relation to finite heat conductivity and finite molecular viscosity.

Analytical solutions of the eigenvalue equation have been given which allow one to identify the different characteristic waves.

Real and imaginary parts of the eigenvalues of the characteristic wave modes have been calculated numerically. Through the use of these eigenvalues the general behavior of the different wave modes has been discussed in detail. The main results are the following:

a. Under the influence of heat conduction, viscosity and ion drag acoustic-gravity waves become dissipative waves. Part of the wave energy is transferred into internal energy of the surrounding gas. This energy dissipation depends on angle of incidence, parameters of the atmosphere and frequency. In the gravity wave range there exists an attenuation minimum at a certain angle of incidence. The atmosphere therefore behaves like a frequency and height dependent selective filter with respect to gravity waves.

b. Under the influence of Coriolis force and ion drag the atmosphere behaves like an anisotropic medium. East to west propagation characteristics of gravity waves differ from north to south propagation characteristics. Ion drag tends to reduce the influence of the Coriolis force.

c. Within the gravity wave range and at altitudes below 500 km viscosity waves are nearly uncoupled from gravity waves and heat conduction waves. The coefficient of viscosity therefore can be neglected in the treatment of gravity waves at thermospheric heights.

ACKNOWLEDGEMENT

I am very indebted to H. G. Mayr for valuable discussions. I would also like to thank very much an anonymous referee for his detailed and important comments.

REFERENCES

K. G. Budden, "Radio waves in the ionosphere," University Press, Cambridge, 1961.

S. Chapman and T. G. Cowling, "The mathematical treatment of non-uniform gases," University Press, Cambridge, 1959.

CIRA, 1965, "COSPAR international reference atmosphere, 1965," North Holland Publishing Company, Amsterdam, 1965.

C. Eckart, "Hydrodynamics of the oceans and the atmosphere," Pergamon Press, Oxford, London, New York, 1960.

T. M. Georges, "HF-Doppler studies of traveling ionospheric disturbances," AGARD XIII Symposium of Phase and Frequency Instability in Electromagnetic Wave Propagation, Ankara, Turkey, October, 1967.

J. Harris and W. Priester, "Time dependent structure of the upper atmosphere," J. Atm. Sci. 19, (1962), 286-301.

C. O. Hines, "Internal gravity waves at ionospheric heights," Can. Journ. Phys. 38, (1960), 1441-1481.

J. E. Midgley and H. B. Liehmon, "Gravity waves in a realistic atmosphere," Journ. Geophys. Res. 71, (1966), 3729-3748.

G. P. Newton, D. T. Pelz and H. Volland, "Direct, in situ observations of wave propagation in the neutral thermosphere," submitted to J. Geophys. Res., 1968.

M. L. V. Pitteway and C. O. Hines, "The viscous damping of atmospheric gravity waves," Can. Journ. Phys. 41, (1963), 1935-1948.

G. D. Thome, "Incoherent scatter observation of traveling ionospheric disturbances," J. Geophys. Res. 69, (1964), 4047-4049.

H. Volland, "Heat conduction waves in the upper atmosphere," Journ. Geophys. Res. 72, (1967), 2831-2841.

H. Volland, "Full wave calculations of thermospheric neutral air motions," submitted to Journ. Geophys. Res. (1968).